Colloid and Polymer Science (2018) 296:809–817
https://doi.org/10.1007/s00396-018-4304-0

ORIGINAL CONTRIBUTION

Molecular interactions between Pluronic F127 and the peptide tritrpticin in aqueous solution

Luiz C. Salay[1] · Elielma A. Prazeres[1] · Nélida S. Marín Huachaca[2] · Monique Lemos[3] · Julia P. Piccoli[4] · Paulo R. S. Sanches[4] · Eduardo M. Cilli[4] · Rubens S. Santos[1] · Eloi Feitosa[3]

Received: 12 January 2018 / Revised: 13 February 2018 / Accepted: 5 March 2018 / Published online: 13 March 2018

Abstract

Triblock copolymers, such as Pluronic F127 (F127), are pharmaceutically important amphiphilic compounds that self-assemble in aqueous solution either as discrete or entangled micelles, depending on their concentration and temperature, which may function as drug delivery vehicle. Herein, we have synthesized the antimicrobial peptide tritrpticin (TRP3), a tryptophan (Trp)- and arginine (Arg)-rich peptide, sequence VRRFPWWWPFLRR, with a broad spectrum of action against bacteria and fungi, to investigate its interaction with F127 in dilute aqueous solution, by using fluorescence and circular dichroism spectroscopies, differential scanning calorimetry, dynamic light scattering, and zeta potential methods. The combined results indicate that at 50 μmol L^{-1} TRP3 and up to 700 μmol L^{-1} F127, these compounds interact together to form F127-bound complexes with the peptide at low concentrations, and immobilized TPR3-containing micelle-like structures at higher concentrations. The F127-TRP3 complexes are stable with varying hydrodynamic size depending on the relative amount of F127, which can be tuned smaller by adjusting the copolymer concentration to values suitable for drug delivery applications in biomedicine.

Keywords Molecular interactions · Peptide · Tritrpticin · Pluronic F127 · Triblock copolymer · Micellization

Introduction

The issue of microbial resistance is a growing problem in the modern society [1]. Antimicrobial peptides from animal and vegetal sources are potential candidates as novel antibacterial, antifungal, and even as antiviral and antitumor agents [1–3]. Particularly interesting are the Trp- and Arg-rich antimicrobial peptides [4, 5]. In special, the cationic 13-residue peptide tritrpticin (TRP3), sequence VRRFPWWWPFLRR, is a cathelicidin with high Arg (30%), Trp (23%), and Pro (15%) content. The high Arg and Trp content, together with the existing three consecutive Trp residues (W^6,W^7,W^8), make this peptide a singular cationic amphiphilic biomolecule [4–6]. TRP3 has high antimicrobial activity acting against both Gram-negative and Gram-positive bacteria, and some fungi [7–9]. In solution, TRP3 interconverts between different conformations, but in the presence of sodium dodecyl sulfate (SDS) micelles, it acquires a conformation with two adjacent turns around Pro^5 and Pro^9 [10]. Such a positioning of the amino acid residues causes TRP3 to adopt an amphipathic turn-turn structure, with the three Trp clustered together and buried in the hydrophobic core of the micelles and the Arg residues on the opposite side of the structure [10]. The mechanism of action of TRP3 has been investigated in micelles [11, 12] and in lipid membranes and liposomes [13–15]; particularly in planar lipid bilayers, TRP3 was found to have a prominent and consistent ion channel-like activity [16]. Moreover, head group specificity for TRP3 interaction with lipid membranes [17] and the effect of membrane curvature on binding of TRP3 has been investigated [18]. Pre-clinical application of

✉ Luiz C. Salay
lcsalay@uesc.br; lcsalay@yahoo.com.br

[1] Department of Exact and Technological Sciences, State University of Santa Cruz–UESC, Ilhéus, BA 45662-900, Brazil

[2] Department of Biological Sciences, State University of Santa Cruz–UESC, Ilhéus, BA 45662-900, Brazil

[3] Department of Physics, São Paulo State University-UNESP, São José do Rio Preto, SP 15054-000, Brazil

[4] Department of Biochemistry and Chemical Technology, Institute of Chemistry, São Paulo State University-UNESP, Araraquara, SP 14800-060, Brazil

native TRP3 has been done [9], and a potential clinical use through the improvement of the peptide's membrane selectivity through re-design has been performed [19]. Tritrpticin also displayed the ability to adsorb on solid and liquid surfaces, and the adsorption process was controlled by ion-specific action making it a potential candidate for the design of nanostructured biointerfaces [20].

Another important issue is how to deliver a drug by minimizing its enzymatic degradation, reducing its deleterious action due to excessive amount of the bioactive agent, typically when administering drugs parenterally, and improving the general therapeutic index, to maximizing the benefits to the patient. An interesting methodology to improve drug administration is the use of delivery vehicles. The triblock copolymer Pluronic F127 (F127) has been used for this purpose [21]. F127 is a nonionic symmetric amphiphile formed by two hydrophilic poly(ethylene oxide) $(EO)_{97}$ sequences bound covalently to the terminals of a hydrophobic poly(propylene oxide) $(PO)_{69}$ sequence, displaying a linear structure $(EO)_{97}$-$(PO)_{69}$-$(EO)_{97}$. These copolymers self-assemble into polymeric micelles containing a PO hydrophobic core surrounded by an EO corona facing the water moiety, where small drugs can be solubilized in [21, 22] or, alternatively, the drug can be conjugated to the micelle-forming polymer [23]. In water, at higher concentrations or temperature, F127 can also assemble as a thermo-reversible gel [24]. This property allows the copolymer to be used as a delivery vehicle for most administrative routes [21, 25–29].

In this work, it was aimed to acquire an insight of the interaction between the peptide TRP3 and F127 in aqueous buffered solution by employing fluorescence spectroscopy, circular dichroism spectroscopy, differential scanning calorimetry, dynamic light scattering, and zeta potential techniques.

Materials and methods

Materials

Pluronic F127, citric acid, monobasic potassium phosphate, boric acid, and acrylamide were acquired from Sigma-Aldrich Co. (St. Louis, USA). Milli-Q water (resistivity 18.2 MΩ cm) was used throughout. All reagents were analytical grade.

Peptide synthesis

Tritrpticin was synthesized manually according to the standard N^{α}-Fmoc protecting-group strategy [30]. The side-chain protecting group Boc (t-butoxycarbonyl) was used for the amino acid W, and (2,2,4,6,7-pentamethyl-dihydrobenzofuran-5-sulfonyl) (Pbf) was used for the amino acid R. The Fmoc-Arg-(Pmc)-Wang resin, which provides a peptide carboxylic acid after cleavage, was employed. The successive α-amino group deprotection and neutralization steps were performed in 20% piperidine/dimethylformamide (DMF) for 20 min. The amino acids were coupled at twofold excess using diisopropylcarbodiimide (DIC)/N-hydroxybenzotriazole (HOBt) in 50% (*v*/*v*) DCM (methylene chloride)/DMF and, if necessary, 2-(1H-benzotriazole-1-yil)-1,1,3,3-tetramethyluroniumhexafluorophosphate (TBTU)/HOBt/diisopropylethyl-amine (DIEA) in 50% (*v*/*v*) DCM/N-methylpyrrolidone (NMP). After a 2-h coupling, the ninhydrin test was performed to estimate the completeness of the reaction. Cleavage from the resin and removal of the side-chain protecting groups were simultaneously performed with reagent K (82.5% TFA, 5% thioanisole, 2.5% ethanedithiol, and 5% water) for 2 h [31]. After this procedure, the crude peptides were precipitated with anhydrous ethyl ether, separated from soluble non-peptide material by centrifugation, extracted into 0.045% (*v*/*v*) TFA/H_2O (solvent A), and lyophilized.

The crude peptides were dissolved in solvent A and purified by semi-preparative HPLC on a Shimadzu system (Japan) using a reverse phase C_{18} column with a linear gradient 20–50% of solvent B (0.036% (*v*/*v*) TFA/acetonitrile) for 90 min. The flow rate was 5 mL/min. UV detection was carried out at 220 nm. The peptide homogeneity was checked by analytical HPLC (Varian, USA), using solvents A and B with a linear gradient of 5–95% (*v*/*v*) of solvent B for 30 min, at a flow rate of 1.5 mL/min and UV detection at 220 nm. The identity of the peptide was confirmed by electrospray mass spectrometry on a ZMD model apparatus (Micromass, UK) and amino acid analysis (Shimadzu model LC-10A/C-47A, Japan).

Sample preparation

F127 and TRP3 peptide solution were prepared in 5 mmol L^{-1} phosphate-borate-citrate (PBC) buffer pH 7.4, at concentrations suitable for each experiment.

Fluorescence spectroscopy

Fluorescence measurements were done using a Shimadzu spectrofluorometer, model RF-5301PC. It was used as a cuvette with an optical path length of 0.2 cm. Excitation and emission slits of 3 nm were used. Intrinsic Trp fluorescence of TRP3 was measured before and after the addition of F127 to a fixed peptide concentration. The TRP3-F127 interaction was supported by changes in the accessibility of the peptide to the aqueous quencher acrylamide on the addition of F127. The experiments were carried out by adding aliquots of a concentrated (2 mol L^{-1}) acrylamide solution to the peptide solution (400 μL) in the absence and in the presence of F127. For the titration, it was added with 1–2.5 μL acrylamide aliquots. The excitation wavelength was 280 nm, and the fluorescence

intensities were monitored after each addition of acrylamide. For the anisotropy measurements, the excitation wavelength was also 280 nm and two polarizers were used to polarize the emission and the excitation light. All fluorescence experiments were carried out at 25 °C.

Circular dichroism

Circular dichroism (CD) spectra were obtained using a spectropolarimeter JASCO, model J-815, coupled to a Peltier temperature control system, model PFD-425S. The spectra were obtained by performing six scans at 25 °C, in the wavelength range 190–250 nm, and using a quartz cuvette. The CD spectra were obtained for the TRP3 solution at 20 μmol L^{-1} in the absence and in the presence of F127 at different concentrations in 5 mmol L^{-1} PBC buffer, pH 7.4.

Differential scanning calorimetry

Differential scanning calorimetry (DSC) measurements were done for different concentrations of F127 in the absence and in the presence of TRP3 at 50 μmol L^{-1}. A VP-DSC microcalorimeter (Microcal Inc., Northampton, MA, USA) was used to collect data, and the Origin® software 7.0 supplied by the manufacturer was used to record and to analyze the data. The experiments were performed by heating and cooling the same volume of the sample and the reference (solvent) at the desired rate scan in the temperature range 1–80 °C. During the heating or cooling procedures, the instrument adds or removes heat to or from the sample or reference to keep them at the same temperature. The added or removed heat was displayed as a function of the temperature (thermogram).

Dynamic light scattering

Dynamic light scattering (DLS) measurements were performed using a light scattering setup (Brookhaven Instruments Corporation, Holtsville, USA), equipped with an adjustable 15-mW maximum power He-Ne laser (wavelength 633 nm), to obtain the hydrodynamic diameter (D_H) of F127 aggregates at varying concentrations in the absence and in the presence of the TRP3 at 50 μmol L^{-1}. The data were collected at the scattering angle $\theta = 90°$ and temperature of 25 °C. From the translational diffusion coefficients, the hydrodynamic diameter was obtained through the well-known Stokes–Einstein relation [32].

Zeta potential measurements

The zeta potentials (ζ) of the F127-containing systems at different concentrations in the absence and in the presence of the TRP3 at 50 μmol L^{-1} were measured using a dynamic electrophoretic light scattering equipment (ZetaPals, Brookhaven Instruments Corporation, Holtsville, USA) equipped with a 632.8-nm He-Ne laser operating at 35 mW. During the scattering measurements, a 6.46-V cm^{-1} electric field was applied to the sample and the electrophorectic mobility determined. The zeta potential was then calculated within the Helmholtz–Smoluchowski approach [33].

Results and discussion

The F127-TRP3 interaction was investigated by fluorescence and circular dichroism spectroscopies, differential scanning calorimetry, and dynamic light scattering and electrophoretic dynamic light scattering techniques. The data are presented and discussed next.

Fluorescence spectroscopy characterization

Figure 1a shows a small increase of TRP3's fluorescence intensity for the lower F127 concentrations and more pronounced increase at higher Pluronic concentrations. In addition, there is a decrease of the of maximum emission wavelength values, indicating blue shift effects, thus showing the partition of TRP3 to a more hydrophobic environment. These data together indicate interaction of the peptide with the polymeric aggregates.

Figure 1b shows the peptide's relative fluorescence intensity (F/F_o) as a function of the F127 concentration, where F_o and F account, respectively, for the fluorescence intensity in the absence and presence of F127. Accordingly, if the increase of an F127 concentration is beyond *ca* 250 μmol L^{-1}, there is a pronounced increase in fluorescence until a plateau was attained past *ca* 500 μmol L^{-1}, which can be ascribed to the critical micellar concentration (CMC) for the F127, at the experiment temperature 25 °C. There are, however, conflicting CMC values for F127 reported in the literature obtained through different methods, solvent and temperature conditions, as well as different manufacturers and batch [34]. This may be probably due to the degree of purity of the product supplied by different manufacturers. Fluorescence spectroscopy studies have shown that the CMC of F127 depends on the temperature. For example, at 30 and 35 °C, CMC equals 2.23×10^{-5} and 1.03×10^{-5} mol kg^{-1}, respectively [34]. Overall, the temperature, above which F127 micelles are formed, displays an inverse dependence on the F127 (logarithmic) composition, as demonstrated by Lin and Alexandridis [35].

It was then investigated the accessibility of the Trp fluorophores of TRP3 to the acrylamide added to the buffered solution by fluorescence quenching tests performed in the presence of F127, as illustrated in Fig. 2, which shows that the quencher effects increase with increasing the amount of added acrylamide. The Stern-Volmer constant (*K*sv) was

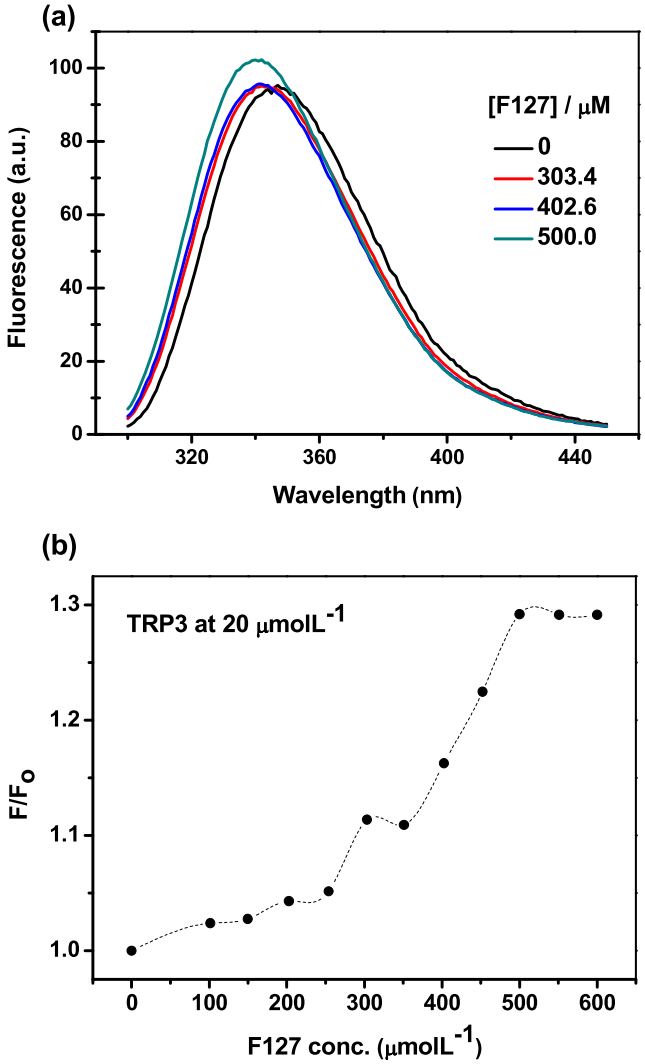

Fig. 1 **a** Effect of an F127 concentration on the fluorescence spectra of TRP3. **b** Relative fluorescence (F/F_0) of TRP3 at 20 μmol L^{-1} in the presence of varying F127. TRP3, buffer PBC 5 mmol L^{-1}, pH 7.4, λ_{exc} 280 nm, slit 3 nm, and sample temperature 25 °C. The dashed line connecting the points in the Fig. 1b is a guide for the eye

calculated from the F_0/F data and expressed as a function of an acrylamide concentration (Fig. 3); here, F_0 and F are respectively the fluorescence intensities in the absence and in the presence of the quencher [36, 37]. The *K*sv values obtained for TRP3 were 4.2 and 1.3 M^{-1} in the absence and in the presence of the F127, respectively. The higher value of K_{SV} shows that there was greater suppression of the peptide fluorescence in the absence than in the presence of F127, indicating that the peptide interacts with F127, most probably being solubilized in the inner core of the polymeric aggregates rich in PO. These K_{SV} values give information about accessibility of the suppressor to the fluorescence molecule; the lower the K_{sv} value, the lower the accessibility of the quencher. Therefore, $K_{sv} = 1.3$ M^{-1} indicates that the Trp residues is being protected from suppression by the interaction of TRP3 with the F127 molecular clusters.

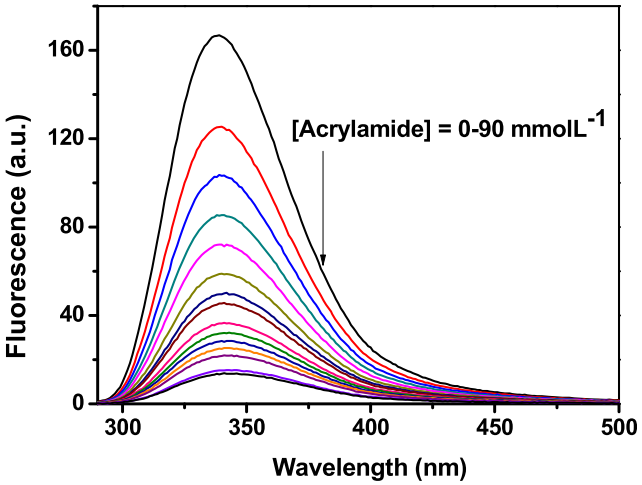

Fig. 2 Fluorescence spectra of TRP3 at 20 μmol L^{-1} mixed with F127 at 350 μmol L^{-1} in the presence of acrylamide. [Acrylamide] = 0, 4.7, 9.4, 14.0, 18.7, 23.3, 27.9, 32.5, 37.0, 41.6, 46.1, 55.0, 63.9, 81.4, and 90.0 mmol L^{-1}. Sample temperature was 25 °C

Fluorescence anisotropy (*r*) tests were performed here to confirm the peptide interaction with F127 aggregates. This technique supplies information mainly about the rigidity of molecular environments. When tritrpticin is in aqueous solution, $r = 0.01877$, while in the presence of F127, $r = 0.04498$. Since *r* is related to the rotational diffusion motion of the fluorescence probe, in solution, *r* approaches zero, while in the presence of F127, *r* is larger indicating that the peptide is in a denser medium, thus confirming the fluorescence intensity data (Fig. 2), which indicate that TRP3 is less flexible due to the interaction with F127 in the copolymer assembly.

Our results are in line with those for tritrpticin in sodium dodecyl sulfate micelles [10], which displayed similar fluorescence effects with a blue shift displacement and an increase of

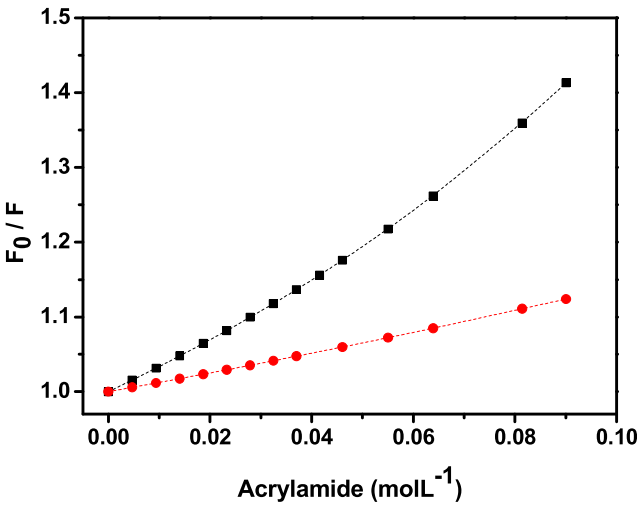

Fig. 3 Relative fluorescence of TRP3 at 20 μmol L^{-1} in solution (black) and in the presence of F127 at 350 μmol L^{-1} (red), as a function of the acrylamide concentration. Sample temperature was 25 °C. The lines connecting the points are guides for the eye

fluorescence intensity on the addition of the surfactant (F127 or SDS) to the peptide solution. In addition, the quenching experiments with acrylamide showed that in the presence of F127 or SDS, TRP3 suffered little quenching effects, indicating that the Trp residues are solubilized inside the copolymer aggregates or micelles. The fluorescence emission of the indole ring of Trp is highly sensitive to the polarity of its environment. Exposure of the Trp to the solvent increases the solvent relaxation and thus the energy of the emitted light decreases, and the maximum emission wavelength shifts to the blue. That is, when Trp is in contact with the aqueous solvent, its energy is reabsorbed by the surrounding water molecules, resulting in lower energetic emission, such as decrease in fluorescence intensity or shift of the maximum emission of fluorescence to red. When Trp is in an environment less exposed to the aqueous solution, i.e., in a more hydrophobic environment, it would exhibit higher energy emission and its maximum fluorescence emission could be shifted to blue. In this case, the tritrpticin may be interacting with the hydrophobic part of the Pluronic. The peptide showed a maximum fluorescence emission length at 347 nm. In the presence of 500 μM Pluronic, this wavelength was 342 nm. The shift to blue was 5 nm. So, the decrease of 5 nm of the wavelength for the maximum emission in the presence of Pluronic clearly indicates that TRP3 peptide went to a more hydrophobic environment. From Figs. 2 and 3, it can be realized that in the presence of acrylamide and F127, there was a pronounced reduction in the fluorescence signal, suggesting that the Trp amino acids of tritrpticin interact with the F127, lying probably at the interface between the polar ethylene oxide (EO) (corona) moiety and the hydrophobic PO core of the copolymer aggregates, protected from the aqueous media. Confocal microscopy studies corroborate these results by showing that TRP3 does not penetrate deeper inside *E. coli* and *S. aureus* cells keeping anchored at the membrane interface [38]. Our fluorescence studies indicate that the three Trp residues (W^6,W^7,W^8) of the central part of tritrpticin remain at the PO/EO interface, as it is at the micelle surface for ordinary surfactants, such as SDS [18].

Circular dichroism spectroscopy characterization

The conformational and structural changes of the tritrpticin in the presence and absence of F127 were also investigated here by circular dichroism spectroscopy, in the ultraviolet (180–250 nm) region. In Fig. 4, the CD spectra of tritrpticin are shown in the absence and presence of F127 at different concentrations. The interpretation of the CD spectra of tritrpticin may be complicated by the presence of multiple aromatic side chains, which prevents a detailed analysis of the secondary structure. However, the characteristic spectrum of neat tritrpticin solution shows a negative ellipticity band at 185 nm, typical for a random structure [10]. The Trp side chain contributes to the CD spectrum approximately between 200 and 225 nm [13, 39].

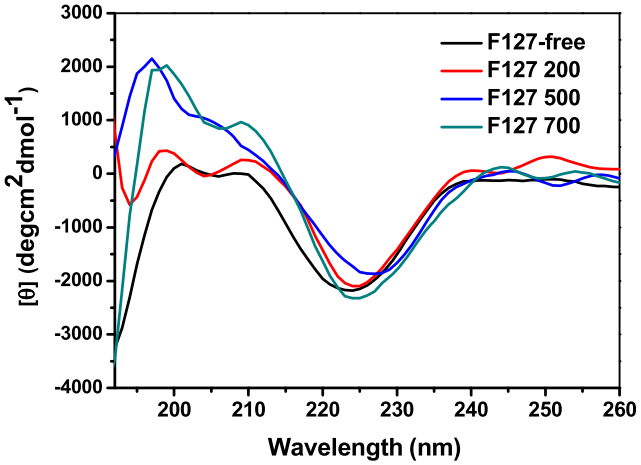

Fig. 4 CD Spectra of TRP3 at 50 μmol L^{-1} in the absence and presence of F127 at 200, 500, and 700 μmol L^{-1}, as indicated. Sample temperature was 25 °C

The presence of a negative band at 225 nm, characteristic of tritrpticin, is in agreement with results reported by other research groups [10, 11, 13, 18]. It can also be noticed that the increase in an F127 concentration caused a change in the spectral profile of TRP3, and the 225 nm band was red shifted; the intensity of the negative band at 185 nm, on the other and, increased significantly, and it was blue shifted, suggesting that the peptide experiences conformational changes in the presence of F127. These data also indicate F127-TRP3 interaction, due to solubilization of the peptide into the copolymer aggregates.

Differential scanning calorimetry characterization

Differential scanning calorimetry technique measures the heat capacity (ΔC_p) to keep the sample and the reference (solvent) temperature the same while the temperature varies at constant heating or cooling rate. ΔC_p reflects the change in the enthalpy of internal energy processes of the sample molecules, displayed as DSC thermograms, or ΔC_p vs. temperature curves [40]. DSC allows one to determine the critical micellar temperature (CMT) and enthalpy (ΔH) of F127 solution in the absence and presence of tritrpticin. It can be used also to investigate the thermotropic behavior of natural or synthetic macromolecules, for example, to determine the denaturation temperature of the protein [41]. The values of CMT and ΔH for F127 and F127-TRP3 aggregates reported here agree well with those for similar systems found in the literature [40, 42, 43]. The values of denaturation temperature (T_d) and enthalpy (ΔH_d) for neat TRP3 solution, to our knowledge, have not been reported so far. Andrushchenko and cols. [44], who investigated lipid-peptide interactions for different compounds at 23 °C, reported that at this temperature, the peptides studied

(including tritrpticin) are not denatured, while the lipids may be either in the gel or in the liquid-crystalline state. This indicates that the actual T_d value of TRP3 is higher than 23 °C, in line with the T_d value of 27.5 °C reported here.

The DSC thermograms of neat F127 solution in the concentration range 70–450 μmol.L^{-1} (Fig. 5a) present a single endothermic event around CMT, with enthalpy ΔH, which decreases exponentially with a concentration [40]. Such a band is characteristic of the reversible formation of micelles upon increase in temperature around CMT [40, 42]. Consecutive heating and cooling of an F127 sample give identical but inverted thermogram profiles, presenting, respectively, in the heating and cooling, a single asymmetric endothermic and exothermic peak around the CMT [40]. The absence of thermal hysteresis in a heating/cooling cycle is an indication of reversible micellization process [40]. The CMT corresponds to the temperature at which the endothermic peak reaches the maximum value [43]. According to Fig. 5a, at 70 μmol L^{-1} F127, the CMT peak cannot be clearly distinguished and the trace resembles a noise signal, while at

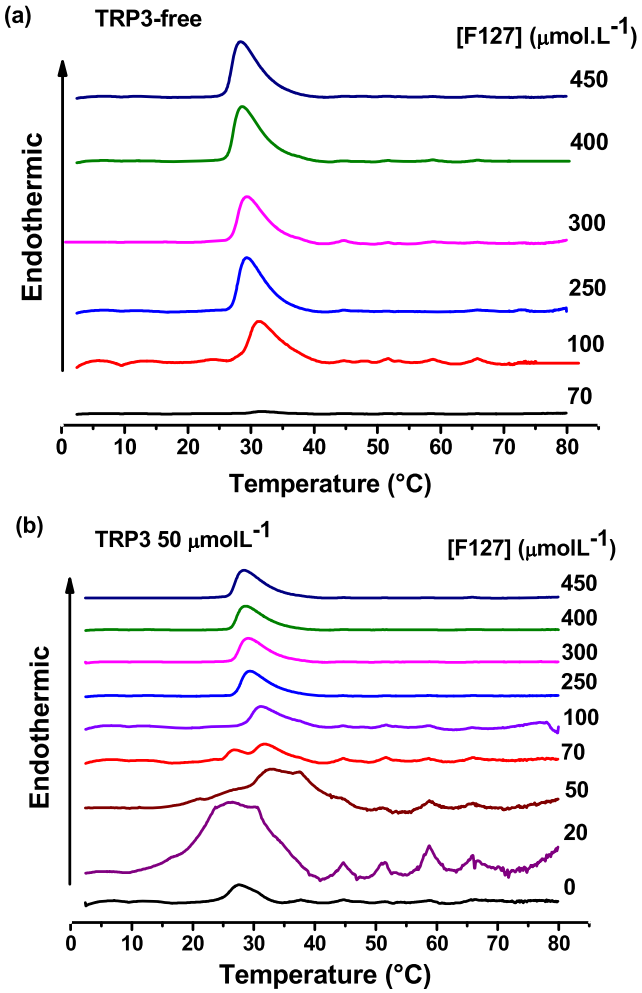

Fig. 5 Heating DSC thermograms of F127 at varying concentrations in the absence (**a**) and presence (**b**) of TRP3 at 50 μmol L^{-1}

100 μmol L^{-1}, the CMT transition appears together with some noise above ca 45 °C. Above this concentration, the noise signal is minimal and the band is shifted to lower temperature, indicating that the CMT decreases with increasing the F127 concentration, as expected [40].

Figure 5b shows DSC thermograms of F127 at concentrations up to 450 μmol L^{-1} in the presence of 50 μmol L^{-1} TRP3. Accordingly, the DSC curve of F127-free TRP3 at 50 μmol L^{-1} displays an endothermic event around T_d = 27.5 °C and enthalpy ΔH_d = 198.2 kJ mol^{-1}, characteristic of the peptide denaturation. In the presence of TRP3, it can be distinguished as two regions (Fig. 5b). Below 100 μmol L^{-1} F127, the thermograms display a broad overlapped endotherm centered at a position (critical temperature) clearly dependent on the F127 concentration, together with some noise characteristics of low concentrate F127 solution. At the lowest F127 concentration (20 μmol L^{-1}), the broad peak maximum is closer to T_d = 27.5 °C (denaturation temperature) of neat TRP3, while at 50 μmol L^{-1}, the peak maximum approaches the CMT value of F127. These indicate that F127 monomers interact with TRP3 leaving it more protected against denaturation, since it requires more energy to denature compared to the free peptide. Above 70 μmol L^{-1}, the peak characteristic of F127 becomes similar to those of TRP3-free, indicating the incorporated peptide does not affect the characteristics of the copolymer aggregates, while the complexed peptide is immobilized and, therefore, protected against denaturation. At the equimolar condition (50 μmol L^{-1}), neither the denaturation nor the micellization peak can be discerned, but instead, an overlap of these two peaks. It means that below this concentration, the peptide (denaturation) transition dominates, while above it, the copolymer (CMT) transition dominates the thermogram profile, thus indicating F127 monomers bound to the peptide and peptides bound to F127 aggregates, respectively, below and above the equimolar concentration.

The CMT and ΔH values of neat F127 solution vary with the copolymer concentration, as shown in Fig. 6. Accordingly, there is a marked decrease in CMT with an increasing F127 concentration in agreement with previous publication for neat F127 [40]. Figure 6 also shows that ΔH of neat F127 increases slightly above 100 μmol L^{-1} with increasing the F127 concentration, attaining at higher concentrations similar value than in the presence of TRP3, which remains roughly constant in the presence of increasing amount of F127.

Similar behavior was also seen for F127 in the presence of TRP3, meaning that the incorporation of the peptide preserves the structure of the copolymer aggregates, in agreement with the above mentioned fluorescence data. Figure 6 also shows that ΔH of neat (TRP3-free) F127 increases slightly with the increase of copolymer concentration. This means that by increasing the F127 concentration, more energy is involved in the formation of micelles due to formation of larger structures, as confirmed by the scattering results shown below.

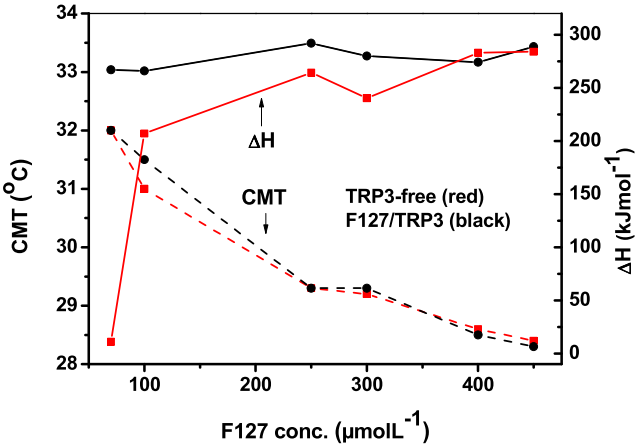

Fig. 6 CMT and ΔH as a function of F127 concentration, in the absence and presence of TRP3 at 50 μmol L^{-1}, as indicated. Data obtained from the analyses of the thermograms in Fig. 5. The lines connecting the points are guides for the eye

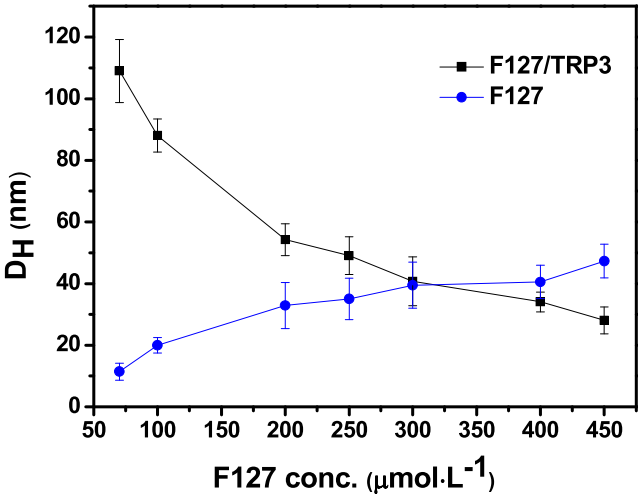

Fig. 7 Hydrodynamic diameter (D_H) of F127 copolymer aggregates as a function of concentration, in the absence (blue) and in the presence (black) of TRP3 at 50 μmol L^{-1}. Data obtained at 25 °C. The lines connecting the points are guides for the eye

Overall, the F127-TRP3 interactions affect significantly the thermogram profile of F127 at concentrations below but not above ca 100 μmol L^{-1} (Fig. 5b). At higher F127 concentrations, however, in the presence of TRP3, the thermograms resemble those of the neat F127 thermograms (Fig. 5a), despite the incorporation of the peptide into the aggregates. Therefore, as TRP3 does not change considerably the CMT and ΔH values of F127 (Fig. 6), the incorporated peptide preserves the F127 aggregate structure and, alternatively, the immobilized peptide structure is protected against denaturation.

Dynamic light scattering measurements

The colloidal stability of the F127 aggregates in the presence and absence of tritrpticin was also investigated by dynamic light scattering in order to determine the hydrodynamic diameter (Fig. 7).

Overall, D_H of the F127 aggregates obtained at 25 °C in the absence of TRP3 increases from ca 10 to 50 nm with increasing the F127 concentration from ca 70 to 450 μmol L^{-1}. Such an increase is expected due to a trend of the Pluronic to form a larger aggregate at a higher concentration [45]. It is worth noticing that this temperature (25 °C) is below the CMT and, therefore, the F127 aggregates might be pre-micellar structures.

The interaction of tritrpticin with F127 at different concentrations results in pronounced initial increase in D_H relative to neat F127 aggregate size. However, D_H decreases from ca 110 to ca 22 nm when the F127 concentration was augmented from ca 70 to 450 μmol L^{-1}. Such a behavior can be explained by the different ways F127 and TRP3 associate to form the colloidal complexes. Initially, up to 100 μmol L^{-1}, there is formation of F127-bound complexes with TRP3, followed by formation of TRP3-containing F127 aggregates with a decreasing amount of TRP3 incorporated (due to the increasing number of aggregates formed with increasing F127 concentration. Such a change in size has implication in the zeta potential of the complexes so formed, as shown next. Note that around 300 μmol L^{-1} F127, the neat F127 aggregates and the F127-TRP3 complexes display similar size.

To our knowledge, there is no record in the literature on the size of the F127-tritrpticin complexes. D_H of neat F127 aggregates in aqueous solution remains constant at 20.4 nm in the temperature range 35–45 °C [45]. In the presence of three different hydrophobic drugs (ibuprofen, aspirin, and erythromycin), it has been reported also an increase in the size of F127 micelles after encapsulation of these drugs [46]. These authors worked above the CMC of F127, thus obtaining micellar structures with the drugs incorporated in. They also reported that the complex size depends on the drug used; in their case, it varies according to erythromycin > ibuprofen > aspirin. Herein, we demonstrate that the complex size is highly dependent on the relative concentration of the compounds. The increase in size of neat F127 aggregates is due to formation of larger aggregates, while the decrease in size of the F127-TRP3 complexes is due to the initial compaction of the peptide structure followed by the formation of micelle-like structures entrapping the immobilized peptide, which in turn does not denature upon heating.

Zeta potential measurements

Zeta potential (ζ) is an important parameter for describing colloidal systems, as their values relate the stability and help to explain the particle interactions. Suspensions displaying ζ values greater (in modulus) than ± 30 mV indicate higher stability, while those having smaller ζ values may be unstable.

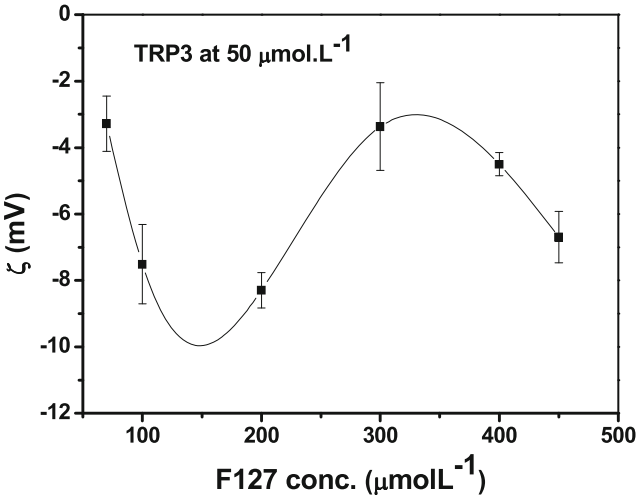

Fig. 8 Zeta potential (ζ) as a function of F127 concentration, in the presence of 50 μmol L^{-1} TRP3. Sample temperature was 25 °C. The line connecting the points is a guide for the eye

There are many factors that affect the zeta potential, such as particle and electrolyte type and concentration, and additives in general [47].

The way ζ of F127-tritrpticin complexes varies with F127concentration is shown in Fig. 8. Accordingly, ζ values fluctuate from ca − 3 to − 9 mV, displaying a mean value of − 6 mV. The low values of ζ may indicate low stability, therefore, suggesting the existence of other (unknown) molecular forces that act on the complexes turning the complexes more stable.

Conclusions

Based on our multi-technique study, the overall conclusion is that the peptide TRP3 interacts with the Pluronic F127 in aqueous solution. As a result, the structure of the F127-TRP3 complexes so formed dependent on the relative amount of Pluronic. At low F127 concentrations, prevail a condensed structure of the F127-bound peptide, while at higher F127 concentrations, the dominating complex structure is micelle-like containing immobilized peptide, which in turn suffer no denaturation when heated above its denaturation temperature, $T_d = 27.5$ °C, as revealed by DSC scans. The so formed complexes may function as drug delivery system for application in nanotechnology.

Acknowledgments E.A.P and R.S.S. thank FAPESB for the master's degree fellowship. M.L. and J.P.P. thank CAPES for the PhD's fellowship. P.R.S.S thanks FAPESP for the PhD's fellowship. N.S.M.H was a CAPES post-doctoral fellow. E.F. and E.M.C. are CNPq research fellows.

Funding information We thank Conselho Nacional de Desenvolvimento Científico e Tecnológico - CNPq (grant number 473885/2012-3) and Fundação de Amparo à Pesquisa do Estado da Bahia - FAPESB (grant number 6769/2011) for the financial support.

Compliance with ethical standards

Conflict of interest The authors declare that they have no conflict of interest.

References

1. Zasloff M (2002) Antimicrobial peptide of multicellular organisms. Nature 415:389–395
2. Mishra B, Reiling S, Zarena D, Wang G (2017) Host defense antimicrobial peptides as antibiotics: design and application strategies. Curr Opin Chem Biol 38:87–96
3. Epand RM, Vogel HJ (1999) Diversity of antimicrobial peptides and their mechanisms of action. Biochim Biophys Acta 1462:11–28
4. Chan DI, Prenner JJ, Vogel HJ (2006) Tryptophan- and arginine-rich antimicrobial peptides: structures and mechanism of action. Biochim Biophys Acta 1758:1184–1202
5. Shagaghi N, Palombo EA, Clayton AH, Bhave M (2016) Archetypal tryptophan-rich antimicrobial peptides: properties and applications. World J Microbiol Biotechnol 32:31
6. Sitaram N (2006) Antimicrobial peptides with unusual amino acid compositions and unusual structures. Curr Med Chem 13:679–696
7. Cirioni O, Giacometti A, Silvestri C, Della Vittoria A, Licci A, Riva A, Scalise G (2006) In vitro activities of tritrpticin alone and in combination with other antimicrobial agents against *Pseudomonas aeruginosa*. Antimicrob Agents Chemother 50:3923–3925
8. Yang ST, Shin SY, Kim YC, Kim Y, Hahm KS, Kim JI (2002) Conformation-dependent antibiotic activity of tritrpticin, a cathelicidin-derived antimicrobial peptide. Biochem Biophys Res Commun 296:1044–1050
9. Ghiselli R, Cirioni O, Giacometti A, Mocchegiani F, Orlando F, Silvestri C, Licci A, Della Vitoria A, Scalise G, Saba V (2006) The cathelicidin-derived tritrpticin enhances the efficacy of ertapenem in experimental rat models of septic shock. Shock 26:195–200
10. Schibli DJ, Hwang PM, Vogel HJ (1999) Structure of the antimicrobial peptide tritrpticin bound to micelles: a distinct membrane-bound peptide fold. Biochemistry 38:16749–16755
11. Andrushchenko VV, Vogel HJ, Prenner EJ (2006) Solvent-dependent structure of two tryptophan-rich antimicrobial peptides and their analogs studies by FTIR and CD spectroscopy. Biochim Biophys Acta 1758:1596–1608
12. Santos TL, Moraes A, Nakaie CR, Almeida FC, Schreier S, Valente AP (2016) Structural and dynamic insights of the interaction between tritrpticin and micelles: an NMR study. Biophys J 111:2676–2688
13. Nagpal S, Gupta V, Kaur KJ, Salunke DM (1999) Structure-function analysis of tritrypticin, and antibacterial peptide of innate immune origin. J Biol Chem 274:23296–23304
14. Schibli DJ, Epand RF, Vogel HJ, Epand RM (2002) Tryptophan-rich antimicrobial peptides: comparative properties and membrane interactions. Biochem Cell Biol 80:667–677
15. Yang ST, Shin SY, Hahm KS, Kim JI (2006) Different modes in antibiotic action of tritrpticin analogs, cathelicidin-derived Trp-rich and Pro/Arg-rich peptides. Biochim Biophys Acta 1758:1580–1586
16. Salay LC, Procopio J, Oliveira E, Nakaie CR, Schreier S (2004) Ion channel-like activity of the antimicrobial peptide tritrpticin in planar lipid bilayers. FEBS Lett 565:171–175
17. Salay LC, Ferreira M, Oliveira ON, Nakaie CR, Schreier S (2012) Headgroup specificity for the interaction of the antimicrobial

peptide tritrpticin with phospholipid Langmuir monolayers. Colloids Surf B: Biointerfaces 100:95–102
18. Bozelli JC, Sasahara ET, Pinto MRS, Nakaie CR, Schreier S (2012) Effect of head group and curvature on binding of the antimicrobial peptide tritrpticin to lipid membranes. Chem Phys Lipids 165:365–373
19. Yang ST, Shin SH, Hahm KS, Kim JI (2006) Design of perfect symmetric Trp-rich peptides with potent and broad-spectrum antimicrobial activities. Int J Antimicrob Agents 27:325–330
20. Salay LC, Petri DF, Nakaie CR, Schreier S (2015) Adsorption of the antimicrobial peptide tritrpticin onto solid and liquid surfaces: ion-specific effects. Biophys Chem 207:128–134
21. Akash MSH, Rehman K (2015) Recent progress in biomedical applications of Pluronic (PF127): pharmaceutical perspectives. J Control Release 209:120–138
22. Kabanov AV, Batrakova EV, Melik-Nubarov NS, Fedoseev NA, Dorodnich TY, Alakhov VY, Chekhonin VP, Nazarova IR, Kabanov VA (1992) A new class of drug carriers: micelles of poly(oxyethylene)–poly(oxypropylene) block copolymers as microcontainers for drug targeting from blood in brain. J Control Release 22:141–158
23. Yokoyama M, Satoh A, Sakurai Y, Okano T, Matsumura Y, Kakizoe T, Kataoka K (1998) Incorporation of water-insoluble anticancer drug into polymeric micelles and control of their particle size. J Control Release 55:219–229
24. Kim SY, Ha JC, Lee YM (2000) Poly(ethylene oxide)-poly(propylene oxide)-poly(ethylene oxide)/poly(ε-caprolactone) (PCL) amphiphilic block copolymeric nanospheres: II. Thermo-responsive drug behaviors. J Control Release 65: 345–358
25. Zhang T, Zhou S, Liu Y, Luo X, Di D, Song Y, Liu X, Deng Y (2017) Polysialic acid and Pluronic F127 mixed polymeric micelles of docetaxel as new approach for enhanced antitumor efficacy. Drug Dev Ind Pharm 26:1–9
26. Yeom DW, Chae BR, Son HY, Kim JH, Chae JS, Song SH, Oh D, Choi YW (2017) Enhanced oral bioavailability of valsartan using a polymer-based supersaturable self-microemulsifying drug delivery system. Int J Nanomedicine 12:3533–3545
27. Mahmoud MO, Aboud HM, Hassan AH, Ali AA, Johnston TP (2017) Transdermal delivery of atorvastatin calcium from novel nanovesicular systems using polyethylene glycol fatty acid esters: ameliorated effect without liver toxicity in poloxamer 407-induced hyperlipidemic rats. J Control Release 254:10–22
28. Chiappetta DA, Hocht C, Opezzo JA, Sosnik A (2013) Intranasal administration of antiretroviral-loaded micelles for anatomical targeting to the brain in HIV. Nanomedicine 8:223–237
29. Al Khateb K, Ozhmukhametova EK, Mussin MN, Seilkhanov SK, Rakhypbekov TK, Lau WM, Khutoryanskiy VV (2016) In situ gelling systems based on Pluronic F127/Pluronic F68 formulations for ocular drug delivery. Int J Pharm 502:70–79
30. Atherton E, Sheppard RC (1989) Solid phase peptide synthesis: a practical approach, I.R.L. Press at Oxford University Press, Oxford
31. King DS, Fields CG, Fields GB (1990) A cleavage method which minimizes side reactions following Fmoc solid phase peptide synthesis. Int J Pep Prot Res 36:255–266
32. Lopes A, Edwards K, Feitosa E (2008) Extruded vesicles of dioctadecyldimethylammonium bromide and chloride investigated by light scattering and cryogenic transmission electron microscopy. J Colloid Interface Sci 322:582–588
33. Delgado AV, González-Caballero F, Hunter RJ, Koopal LK, Lyklema J (2005) Measurement interpretation of electrokinetic phenomena. Pure Appl Chem 77:1753–1805
34. Bandula R, Vasilescu M (2011) Imidazole derivatives as absorption probes for Pluronics core-shell aggregates micropolarity investigation. J Appl Spectrosc 78:209–217
35. Lin Y, Alexandridis P (2002) Temperature-dependent adsorption of Pluronic F127 block copolymers onto carbon black particles dispersed in aqueous media. J Phys Chem B 106:10834–10844
36. Romani AP, Marquezin CA, Ito AS (2010) Fluorescence spectroscopy of small peptides interacting with microheterogeneous micelles. Int J Pharm 383:154–156
37. Romani AP, Marquezin CA, Soares AE, Ito AS (2006) Study of the interaction between *Apis mellifera* venom and micro-heterogeneous systems. J Fluoresc 16:423–430
38. Zhu WL, Lan H, Park Y, Yang ST, Kim JI, Park IS, You HJ, Lee JS, Park YS, Kim Y, Hanm KS, Shin SY (2006) Effects of Pro→ peptoid residue substitution on cell selectivity and mechanism of antibacterial action of tritrpticin-amide antimicrobial peptide. Biochemistry 45: 13007–13017
39. Wood RW (1994) Contributions of tryptophan side chains to the far-ultraviolet circular dichroism of proteins. Eur Biophys J 23: 253–262
40. Feitosa E, Winnik FM (2010) Interaction between Pluronic F127 and dioctadecyldimethylammonium bromide (DODAB) vesicles studied by differential scanning calorimetry. Langmuir 26:17852–17857
41. Johnson CM (2013) Differential scanning calorimetry as a tool for protein folding and stability. Arch Biochem Biophys 531:100–109
42. Alexandridis P, Holzwarth JF (1997) Differential scanning calorimetry investigation of the effect of salts on aqueous solution properties of an amphiphilic block copolymer (poloxamer). Langmuir 13: 6074–6082
43. Chiu MH, Prenner EJ (2011) Differential scanning calorimetry: an invaluable tool for a detailed thermodynamic characterization of macromolecules and their interactions. J Pharm Bioallied Sci 3: 39–59
44. Andrushchenko VV, Vogel HJ, Prenner EJ (2007) Interactions of tryptophan-rich cathelicidin antimicrobial peptides with model membranes studied by differential scanning calorimetry. Biochim Biophys Acta 1768:2447–2458
45. Attwood D, Collett JH, Tait CJ (1985) The micellar properties of the poly(oxyethylene)-poly(oxypropylene) copolymer Pluronic F127 in water and electrolyte solution. Int J Pharm 26:25–33
46. Basak R, Bandyopadhyay R (2013) Encapsulation of hydrophobic drugs in Pluronic F127 micelles: effects of drug hydrophobicity, solution temperature and pH. Langmuir 29:4350–4356
47. Manaia EB, Abuçafy MP, Chiari-Andréo BG, Silva BL, Oshiro Junior JA, Chiavacci LA (2017) Physicochemical characterization of drug nanocarriers. Int J Nanomedicine 12:4991–5011